Published in final edited form as:
Mol Microbiol. 2009 February ; 71(4): 912–924. doi:10.1111/j.1365-2958.2008.06574.x.

Controlled degradation by ClpXP protease tunes the levels of the excision repair protein UvrA to the extent of DNA damage

Mihaela Pruteanu[1,2] and **Tania A. Baker**[1,2,*]

[1]Howard Hughes Medical Institute, Massachusetts Institute of Technology, Cambridge, Massachusetts 02139

[2]Department of Biology, Massachusetts Institute of Technology, Cambridge, Massachusetts 02139

Summary

UV-irradiation damages DNA and activates expression of genes encoding proteins helpful for survival under DNA stress. These proteins are often deleterious in the absence of DNA damage. Here, we investigate mechanisms used to regulate the levels of DNA-repair proteins during recovery by studying control of the nucleotide excision repair (NER) protein UvrA. We show that UvrA is induced after UV-irradiation and reaches maximum levels between ~20 to 120 min post-UV. During post-UV recovery, UvrA levels decrease principally as a result of ClpXP-dependent protein degradation. The rate of UvrA degradation depends on the amount of unrepaired pyrimidine dimers present; this degradation rate is initially slow shortly after UV, but increases as damage is repaired. This increase in UvrA degradation as repair progresses is also influenced by protein-protein interactions. Genetic and in vitro experiments support the conclusion that UvrA-UvrB interactions antagonize degradation. In contrast, Mfd appears to act as an enhancer of UvrA turnover. Thus, our results reveal that a complex network of interactions contribute to tuning the level of UvrA in the cell in response to the extent of DNA damage and nicely mirror findings with excision repair proteins from eukaryotes, which are controlled by proteolysis in a similar manner.

Keywords

ClpXP protease; proteolysis; DNA damage; NER pathway; UvrA protein

INTRODUCTION

Free–living organisms are exposed to diverse environmental (chemical and physical) and endogenous (metabolic products) factors that can damage DNA. Exposure to UV-irradiation, a deleterious environmental factor, produces a variety of photoproducts in the genomic DNA, of which the major species are cyclobutane pyrimidine dimers (CPDs) and pyrimidine-pyrimidone (6-4) photoproducts (6-4PPs) (Cadet *et al.*, 1992). To survive in a UV-rich environment and combat DNA damage, *E.coli* induces the SOS response. Induction occurs via inactivation of the LexA repressor, which results in transcriptional activation of the approximately 40 SOS regulon genes (Walker *et al.*, 2000; Courcelle *et al.*, 2001; Friedberg *et al.*, 2005). Many of these genes encode proteins involved in repair of DNA damage or damage tolerance that enhance survival during exposure to damaging agents. However, these proteins can be deleterious when present at inappropriate levels, especially

*Corresponding author. Mailing address: Massachusetts Institute of Technology, Department of Biology, 68-523, 77 Massachusetts Ave, Cambridge MA 02139. Phone: 617-253-3594, Fax: 617-252-1852, tabaker@mit.edu.

in the absence of damage. We are therefore interested in elucidating mechanisms controlling the levels of SOS-regulon proteins during the recovery phase of a DNA damage response. Numerous SOS proteins are substrates for ATP-dependent proteolysis (Little, 1983; Mizusawa and Gottesman, 1983; Frank *et al.*, 1996; Wu *et al.*, 1999; Gonzalez *et al.*, 2000; Neher *et al.*, 2003a; Neher *et al.*, 2003b; Nagashima *et al.*, 2006; Neher *et al.*, 2006), but little is known about how protein degradation is controlled during the repair and recovery phases of a damage response.

The SOS regulon includes the *uvrA* and *uvrB* genes involved in the nucleotide excision repair (NER) pathway (Kenyon and Walker, 1981; Fernandez De Henestrosa *et al.*, 2000; Courcelle *et al.*, 2001). UV-induced DNA lesions are recognized and removed by the NER pathway through the concerted action of the UvrABC proteins. NER is comprised of two subpathways: global NER and transcription-coupled repair (TCR). During global NER the $UvrA_2UvrB$ or $UvrA_2UvrB_2$ complex recognizes the damaged sites in the DNA (Orren and Sancar, 1989; Theis *et al.*, 2000; Verhoeven *et al.*, 2002; Malta *et al.*, 2007) and recruits the UvrC endonuclease in a multistep ATP-dependent process (Sancar and Rupp, 1983). The UvrAB complex scans the DNA in search of damage, with UvrA detecting a distortion in the DNA and UvrB verifying the presence of the lesion. After the damage is found, UvrA hydrolyzes ATP, dissociates from the complex, and the UvrB-DNA preincision complex is formed. The UvrC endonuclease binds to this preincision complex and cleaves the damaged DNA strand on both sides of the lesion. This ssDNA segment is then removed to allow for repair DNA synthesis (Sancar, 1996; Van Houten *et al.*, 2005; Truglio *et al.*, 2006).

The TCR subpathway requires Mfd, the transcription-coupling repair factor, which recognizes the stalled RNA polymerase at the damaged site and recruits UvrA (Roberts and Park, 2004; Savery, 2007). As in global repair, UvrA loads UvrB onto the damaged DNA to initiate repair. As a consequence of the TCR subpathway, DNA lesions are repaired more efficiently from transcribed strands than from nontranscribed strands in the genome (Mellon and Hanawalt, 1989; Selby and Sancar, 1991; Selby *et al.*, 1991; Mellon, 2005).

NER can repair a broad range of DNA lesions and thus it has been suggested that the UvrAB complex recognizes distortions in the DNA. This idea is supported by the observation that 6-4PPs, which distort the DNA backbone more than CPDs, are incised at a higher rate (Chandrasekhar and Van Houten, 2000). The NER machinery can also attack undamaged DNA and thus may be a source of spontaneous mutations (Caron and Grossman, 1988; Branum *et al.*, 2001; Hasegawa *et al.*, 2008). Therefore, there must exist mechanisms to restrict the activity of the DNA repair proteins, both temporally and spatially, to regions of DNA damage.

In this study we address the strategies *E. coli* uses to return the NER proteins to their basal steady-state levels after DNA damage has been repaired, to avoid promiscuous incision activity on non-damaged DNA. Proteolysis is a powerful mechanism used by cells to control adaptation and recovery after exposure to a variety of stress conditions. *E. coli* has five ATP-dependent proteases: ClpAP, ClpXP, FtsH, HslUV and Lon (Gottesman, 2003; Sauer *et al.*, 2004; Hanson and Whiteheart, 2005). To degrade proteins, ClpX (the ATPase) selects the substrates by recognizing short peptide motifs often near the N or C terminus, then unfolds the proteins and translocates the polypeptides into the ClpP (peptidase) proteolytic chamber where they are cleaved into short peptides (Sauer *et al.*, 2004). Adaptor or delivery proteins facilitate recognition and promote degradation of several substrates by binding to the N-domain of ClpX (Sauer *et al.*, 2004).

A previous proteomic study indicated that UvrA is a substrate for degradation by ClpXP, but did not investigate the physiological context of this degradation (Neher *et al.*, 2006). To

understand the physiological relevance of UvrA degradation we performed experiments to detect changes in UvrA levels and determine how proteolysis changes throughout the repair and recovery phases of the damage response. We found that UvrA levels increase after UV-irradiation (10J/m^2) as a result of induced rate of synthesis and increased protein stability in concert with SOS-induced transcription of *uvrA*. The UvrA levels peak 20 to 120 min post-UV, and during further post-UV recovery the levels gradually decline in wild-type cells but not in *clpX* or *clpP* mutant cells. We show that ClpXP degrades UvrA at different rates during the distinct stages of post-UV recovery when the cells contain different levels of unrepaired CPDs. These data suggest that removal of CPDs significantly enhances the rate of UvrA degradation. As UvrA interacts with both UvrB and Mfd during repair, the influence of these proteins on UvrA degradation was tested. Our results suggest that soon after DNA damage, when repair is most needed, UvrA is stabilized by two types of interactions: complex formation with damaged DNA and protein-protein interactions with its partner in the repair, the enzyme UvrB. Once repair nears completion, these interactions become less frequent, the rate of degradation raises, and UvrA levels fall and eventually reach their pre-induction levels.

RESULTS

UvrA protein levels decrease during post-UV recovery in wild-type cells but not in clpX or clpP mutant cells

Quantitative mass spectrometry experiments suggested that ClpXP recognized UvrA at a detectable level only when cultures were treated with a DNA damaging agent (nalidixic acid) (Neher *et al.*, 2006). We wanted to understand why ClpXP recognizes UvrA under DNA damage-inducing conditions, when UvrA is most needed to repair DNA lesions, and if there was any regulation of this recognition. First, we measured the UvrA levels before and after UV exposure (UV dose 10J/m^2) in wild-type, *clpX* or *clpP* deletion cells, and normalized these levels against the respective values in cells before irradiation. In wild-type cells UvrA levels increased following UV-treatment, and reached a maximum (approximately 2.5-fold increase) between 20 and 120 min post-UV (Fig. 1A). Prolonged recovery resulted in a decrease of UvrA level, with the level returning to that found in undamaged cells approximately 3 hours after UV treatment. A very similar pattern of induction of UvrA and post-UV decline was previously described (Lin *et al.*, 1997). In *clpX* or *clpP* mutant cells the UvrA protein was induced by UV treatment, but no drop in protein level was observed during recovery (Fig. 1A). The mutant cells showed a slight growth defect at long times post-UV (Supplemental Figure 1) and a slightly lower induction of UvrA after UV-damage compared with the induction in wild-type cells (approximately 1.75-fold increase in level versus a 2.5-fold increase). However, maximal induction is reached in the same time frame, regardless of the presence or absence of ClpX or ClpP.

The rate of UvrA degradation varies with recovery time

We reasoned that the post-UV decline in UvrA protein levels in wild-type cells was most likely the result of protein degradation. To determine directly whether UvrA was degraded during the different stages of recovery post-UV, we used pulse-chase labeling of wild-type cells and immunoprecipitation of UvrA (Fig. 2A). In cells that were labeled immediately after UV-irradiation (no recovery) or allowed to recover for 5 min and then labeled, UvrA was degraded with a half-life of ~175 min. Importantly, UvrA degradation was substantially faster (half-life of ~95 min) in cells that were allowed to recover for 15 min after UV damage, and maximal proteolysis (half-life of ~70 min) was observed at recovery time of 40 min. The culture doubling-time after UV-irradiation was about 90 min (Supplemental Figure 1), thus cells rid themselves of UvrA principally by protein degradation rather than by

dilution due to cell growth. The UvrA half-life did not decrease further by increasing the time of recovery (data not shown).

As a control for the degradation activity of ClpXP, we tested the rate of sigmaS degradation (also a ClpXP substrate) in undamaged cells and immediately after UV-irradiation. Under both conditions, sigmaS was degraded with a half-life of 1-2 min (data not shown), which is characteristic for this protein in exponentially growing cells in minimal medium (Lange and Hengge-Aronis, 1994). These results support the assumption that ClpXP activity, *per se*, is not affected by UV treatment.

UvrA synthesis rates vary ten-fold during damage and recovery

In our pulse-chase experiments we observed that UvrA rates of synthesis vary significantly during post-UV recovery (compare the intensities of the UvrA bands in the first lanes of Fig. 2A). Therefore, to analyze the interplay between protein synthesis and protein degradation, we measured the UvrA rate of synthesis before and after DNA damage. In the absence of DNA damage, UvrA was synthesized at low rate (Fig. 2B). During post-UV recovery this rate increased and reached a maximum (tenfold higher than the basal level) at 5-15 min recovery. Further recovery resulted in a gradual decrease in synthesis rate, with return to the basal rate 2 hours after UV-irradiation (Fig. 2B).

The *uvrA* and *uvrB* genes are among the first SOS genes to be induced following UV-irradiation (Kenyon and Walker, 1981; Fernandez De Henestrosa *et al.*, 2000). During post-UV recovery the decline in *uvrA* transcript level and UvrA rate of synthesis, as well as enhanced UvrA proteolysis contribute to return UvrA to the basal level after the DNA damage has been repaired (see *Discussion*).

UvrA protein is stabilized in clpX mutant cells

To determine more directly if UvrA degradation was promoted by ClpXP protease, we repeated the pulse-chase experiments in a *clpX* deletion strain. We choose to determine the rate of UvrA degradation in the mutant cells at 40 min recovery because the fastest rate of degradation was observed at this time point (Fig. 2A). Strikingly, the UvrA half-life increased from ~70 min in wild-type cells to ~275 min in the *clpX* mutant cells (Fig. 3). The UvrA rate of synthesis was also higher in undamaged *clpX* mutant cells than in wild-type cells (data not shown) suggesting that ClpX also helps to keep UvrA levels very low under normal conditions. We propose that ClpX keeps UvrA levels low in at least two different ways: repressing gene expression (likely indirectly) and degrading UvrA.

Stabilization of UvrA in ClpXP-defective cells is not due to a defect in repair

Two general models could explain the stabilizing effect of the *clpX* mutant on UvrA: (1) the effect could be due directly to preventing proteolysis of UvrA by the ClpXP protease and (2) the effect could be more indirectly caused by a higher level of DNA damage or deficiency in DNA repair in the *clpX* mutant cells. As previous studies have revealed that ClpXP influences numerous components of the SOS regulon (see *Introduction*), including the LexA repressor, it was important to directly address the degree to which this second model may be contributing to UvrA stabilization.

To address how much DNA damage was present in the different strains, we needed an assay for UV-induced photoproducts. UV light induces two major types of lesions, CPDs and 6-4PPs (Cadet *et al.*, 1992). The extent of UV damage repair was assayed in wild-type, *clpX* or *clpP* mutant cells by measuring the CPD levels in DNA immediately after UV exposure, and at different time points during recovery of the irradiated cells. CPDs were measured by direct ELISA under conditions where photolyase (another repair enzyme) was inefficient.

As shown in Fig. 4A, CPDs were both induced by UV light and repaired with similar efficiencies in wild-type, *clpX* or *clpP* mutant cells. Approximately 30-34% of the CPDs were removed in cells allowed to recover for 5 min and the extent of DNA repair increased gradually with the time of recovery: ~57-61% were removed by 15 min recovery and ~75-77% by 40 min recovery. This CPD repair in wild-type cells was similar with that reported by Lin *et al.*, 1997. To test whether any of the CPDs were repaired by the photolyase, we measured the removal of CPDs in a *clpX, uvrA* double mutant, and observed no detectable repair (data not shown). These results are consistent with the fact that little blue light (300-500 nm) was present in our experiments, and it is this wavelength light that is used by *E. coli* photolyase to repair the CPDs (Kelner, 1951; Thompson and Sancar, 2002; Cleaver, 2003).

The results from the measurement of CPD levels in wild-type, *clpX* and *clpP* cells clearly revealed that the levels of damage, and kinetics of repair were similar with and without a functional ClpXP protease. These data argue against the model that UvrA is stabilized in the *clpX* mutant due to high levels of DNA lesions in these cells. Given that ClpXP likely directly degrades UvrA, one might have expected faster kinetics of CPD repair in the protease mutant strains. However, examination of UvrA protein levels revealed that the change in protein concentration was not dramatic during the “repair phase” of the damage response. We performed western blots to measure the UvrA levels; in each case, values were normalized against the level in wild-type cells before irradiation. UvrA levels in mutant cells compared to the levels in wild-type cells during recovery were only 1.3-fold higher (Fig. 4B). This rather minor difference in UvrA explains the similar rates of CPDs removal in wild-type and mutant cells during recovery. Note that the protease mutant cells also have a 2-fold higher level of UvrA compared with that in wild-type cells before irradiation (Fig. 4B), explaining the smaller increase in UvrA levels following UV exposure (Fig. 1A) and supporting the hypothesis that UvrA is also a ClpXP substrate during “nondamaging” conditions.

The influence of other NER components on UvrA degradation

During the DNA repair process the UvrA protein interacts with both UvrB and Mfd (Fig. 5A). UvrB consists of five structural domains (see Fig. 5A) (Theis *et al.*, 2000). The crystal structure of *Bacillus caldotenax* UvrB shows that the UvrA-interacting residues are located on the surface of domain 2 (Truglio *et al.*, 2004). Structural analysis of *Bacillus stearothermophilus* UvrA and biochemical experiments reveal that an inserted segment, within the nucleotide-binding domain I of UvrA, interacts with D2 of UvrB (Pakotiprapha *et al.*, 2008). The structure of Mfd was recently solved and reveals eight structural domains (see Fig. 5A), three of which comprise a homology module similar to domains 1a, 2 and 1b of UvrB (Assenmacher *et al.*, 2006;Deaconescu *et al.*, 2006). The putative UvrA binding surface is buried in the D2/D7 interface of Mfd (Deaconescu *et al.*, 2006). Based on the previous experiments with a C-terminal deletion mutant of Mfd, it has been proposed that this region (D7) may play a role in preventing unproductive Mfd-UvrA interactions and UvrA sequestration from the global NER in the absence of the stalled RNA polymerase (Selby and Sancar, 1995;Deaconescu *et al.*, 2006).

To test whether UvrB and Mfd proteins influence UvrA degradation we performed pulse-chase experiments in *uvrB* and *mfd* mutant cells and determined the rate of UvrA degradation at 40 min post-UV treatment. Deletion of either *mfd* or *uvrB* increased UvrA half-life from ~70 min in wild-type cells to ~150 min in the *mfd* mutant and to ~290 min in the *uvrB* mutant cells (Fig. 5B). The absence of Mfd or UvrB from the cells is expected to affect the kinetics of DNA repair and may also influence UvrA stability more directly, as both proteins are known to interact with UvrA.

To begin to differentiate between protein-protein interactions and damaged DNA interactions that may contribute to increased stability of UvrA, we measured CPD removal in the *mfd* and *uvrB* mutants to assess the extent of repair. Interestingly, the *mfd* mutant was able to repair lesions. Although the kinetics of repair were slower, by 40 min recovery these mutant cells had a similar level of CPDs as the wild-type cells (Fig. 5C). However, at this time point, UvrA degradation was clearly repressed (Fig. 5B). Thus, we conclude that the mechanism underlying the increased stability of UvrA in the *mfd* mutant is not simply the persistence of damaged DNA. Rather, the presence of Mfd somehow "enhances" UvrA degradation; possible mechanisms for this enhancement are discussed below (see *Discussion*).

In contrast to the effect of *mfd*, disruption of the *uvrB* gene eliminated the capability of UV-irradiated cells to repair damaged DNA (Fig. 5C). Therefore we next wanted to test if the increased UvrA half-life in the *uvrB* mutant was solely due to the elevated CPDs slowing degradation or if the UvrB protein also plays a direct role in UvrA degradation. To test whether the damaged DNA-UvrA interaction was exclusively responsible for increased UvrA stability, we constructed an inactive *uvrC* allele and measured the rate of UvrA degradation in these cells. This strain should contain all components of the NER pathway but should be unable to repair lesions.

Upon binding to the DNA-UvrB preincision complex, UvrC performs two incisions in a defined order (Sancar, 1996). UvrC contains two distinct active sites that promote these two DNA cleavages (Verhoeven *et al.*, 2000). We decided to construct a chromosomally-inserted *uvrC* alelle that encodes a protein unable to perform the 5' incision, as Cho, another UvrC-like endonuclease, is able to cut the DNA at the 3' side of the lesion (Moolenaar *et al.*, 2002). Using recombineering (Thomason *et al.*, 2007) we constructed an $UvrC^{D399A}$ variant, which carries a replacement at one of the active-site residues (Lin and Sancar, 1992) and measured the rate of UvrA degradation and the removal of CPDs in this strain. At the 40 min recovery time, the half-life of UvrA protein in this mutant strain was ~440 min and only ~15-20% of CPDs were removed (Fig. 5B and C). The cells carrying the inactive UvrC showed a minor difference in the CPD content compared to the CPDs in the *uvrB* mutant cells (Fig. 5C). Interestingly, the UvrA half-life increased from ~290 min in *uvrB* mutant to ~440 min in the $uvrC^{D399A}$ mutant cells. Thus, based on these initial results, we suggest that both elevated CPD content and a UvrB-UvrA interaction may contribute to the increased UvrA stability in cells carrying the inactive UvrC.

To determine more directly the effect of UvrB on UvrA turnover we performed *in vitro* degradation experiments (Fig. 6). UvrA was degraded by ClpXP *in vitro*. Interestingly, the *in vitro* reaction required the presence of undamaged DNA. The rate of degradation was modest, consistent with our *in vivo* results that UvrA is not a rapidly turned-over substrate. Importantly, however, the presence of UvrB *in vitro* completely inhibited UvrA degradation, most likely by its direct interaction with UvrA. Further evidence for this complex formation *in vitro* came from the observation that the cryptic ATPase activity of UvrB was activated in the presence of UvrA (data not shown). Thus, we conclude that UvrB is likely a direct player in stabilizing UvrA via protein-protein contacts, whereas undamaged DNA appears to be an "activator" of UvrA degradation.

DISCUSSION

To ensure survival in a harsh UV-rich environment many organisms use various DNA repair mechanisms, such as the NER pathway, to remove UV-induced lesions. Most of the bacterial NER components are members of the SOS regulon and are induced following exposure to UV light, but little is known about the fate of these proteins during recovery. In

this study we address the strategies *E. coli* uses to return the NER protein, UvrA, to its basal steady-state level as damage repair is completed. ATP-dependent proteases play an important role in diverse stress responses that allow bacteria to survive and recover from DNA damage, starvation, heat shock or oxidative stress (Gottesman, 2003; Jenal and Hengge-Aronis, 2003; Nagashima *et al.*, 2006; Neher *et al.*, 2006). *E. coli* uses three ATP-dependent proteases, ClpXP, Lon and HslUV, for degradation of numerous members of the SOS regulon to restore their basal protein levels after damage repair. Therefore, regulated gene expression and protein turnover cooperate to adjust the protein levels to the cell's needs.

The CPD content appears to determine the fate of UvrA protein

Here we show that UvrA levels peak 20 to 120 min post-UV and decrease during prolonged recovery, reaching the levels found in undamaged cells approximately 3 hours after UV exposure. The decrease of UvrA levels during post-UV recovery is a combined consequence of the decline in CPD content, the changing rate of UvrA synthesis, and enhanced UvrA proteolysis (Fig. 7A). Importantly, we find that UvrA is degraded during post-UV recovery at rates that are correlated with the amount of repaired CPDs in the cells (Fig. 7B). This type of change in degradation rate during a physiological response is likely very useful in the control of biological pathways, but has not been clearly demonstrated in many cases (Frank *et al.*, 1996). With UvrA, the maximum degradation rate is reached by 40 mins post-UV; this is also when the rate of synthesis starts to decline gradually, although synthesis is still nearly 8-fold higher than before damage (Fig. 7A and B). At this time point enhanced degradation appears to function to keep UvrA from accumulating to even higher levels. Notice that in the *clpX* and *clpP* mutants, protein levels continue to rise until 60 min (see Fig. 1). Then, in wild-type cells by the 120 min recovery point, protein levels fall due to decreased synthesis coupled with the maximum degradation rate, until they fall to such a low level that the protein is no longer efficiently recognized by the protease, and the pre-induction level is restored.

A previous study demonstrated that the N-terminally His-tagged UvrA is also degraded in a ClpXP-dependent manner, with a half-life of about 5 min (Neher *et al.*, 2006). There were many differences in the experimental conditions of the previous work and our current study. For example in the previous study: the UvrA was tagged, it was over-expressed from a non-native promoter, the DNA damaging agent was different, the cells were grown in a richer media, and degradation was measured by western after inhibition of protein synthesis, rather than by pulse labeling. We did not systematically analyze what factors accounted for the different degradation rates. However, the presence of additional tags in the proteins carrying natural degradation motifs often enhances protein degradation (Prakash *et al.*, 2004; Hoskins and Wickner, 2006). Expression levels can also have a large effect on *in vivo* degradation rates. Importantly both the native and tagged UvrA were substantially stabilized in a *clpX* mutant strain, strongly implicating ClpXP as the major protease responsible for UvrA degradation. Furthermore, based on *in vitro* degradation (Fig. 6) we suggest that UvrA is a direct ClpXP substrate.

One feature of the *in vitro* degradation reaction gives an exciting hint as to an additional controlling role DNA may play in UvrA stability. We found that undamaged DNA was a necessary cofactor to observe ClpXP-dependent degradation of UvrA *in vitro*. This observation suggests that the form of UvrA that is recognized by ClpXP is that which is bound to undamaged DNA, providing a very simple mechanism by which the cells could sense the UvrA that must be "cleared" from cells to prevent inappropriate targeting of NER to undamaged sites. Thus, DNA may play two opposing roles in UvrA degradation: lesion-containing DNA is stabilizing whereas undamaged DNA appears to be a direct player in stimulating recognition by ClpXP protease.

The UvrA interacting partners differentially regulate UvrA degradation

In the presence of damaged DNA, when repair mechanisms are still necessary, UvrA is protected against degradation, whereas upon removal of CPDs, the rate of UvrA proteolysis increases. UvrB forms a complex with UvrA for proper damage recognition and we show that this protein also plays a role in UvrA stability. Deletion of *uvrB* increases the half-life of UvrA from ~70 min (in wild-type cells at 40 mins recovery) to ~290 min (Fig. 5B). The principle mechanistic basis for this stabilization is probably the increased persistence of damaged DNA-UvrA interactions, since the capability to repair the CPDs is eliminated in this mutant (Fig. 5C). UvrA stability increases further to ~440 min in the $uvrC^{D399A}$ mutant, which also cannot repair DNA lesions (Fig. 5B and C); this mutant strain has all the NER components, including the UvrB protein. An attractive interpretation of these data is that in addition to damaged DNA-UvrA interactions, UvrB protein increases UvrA stability via protein-protein contact. This hypothesis is supported by *in vitro* degradation experiments in which UvrB antagonizes degradation of UvrA by ClpXP (Fig. 6). Therefore, we conclude that during the initial phases of a DNA damage response, UvrA is at least partially protected against degradation by two types of interactions: damaged DNA-UvrA contacts and UvrA-UvrB protein-protein interactions.

UvrA interacts also with Mfd, which recognizes stalled RNA polymerase at the damaged site and recruits UvrA for damage repair (Roberts and Park, 2004). Interestingly, deletion of *mfd* gene increases the UvrA half-life from ~70 min (in wild-type cells) to ~150 min (Fig. 5B) although the mutant cells are able to repair the damaged DNA and have the same CPDs content as the wild-type cells at the 40 min recovery time point (Fig. 5C). Thus, Mfd appears to be, either directly or indirectly, an “enhancer” of UvrA degradation, at least once repair is nearing completion. We speculate that Mfd likely plays two roles in UvrA stability. At early times after damage, when the CPD content is high, Mfd removes stalled RNA polymerase molecules and stabilizes UvrA by recruiting repair factors to the lesion sites. In contrast, after the damage has been repaired, Mfd switches to act as an enhancer of UvrA degradation. Two attractive models for how Mfd may promote UvrA degradation are that (1) it could function directly as a adaptor-protein, enhancing UvrA recognition by ClpXP or that (2) the Mfd-UvrA interaction may expose protease recognition determinants in UvrA protein. Thus, the NER components differentially regulate UvrA degradation: UvrB stabilizes UvrA against degradation, whereas Mfd, at least at late times during recovery appears to promote UvrA degradation.

Regulated degradation also controls nucleotide excision repair in other organisms

Components of the nucleotide excision factors (NEFs) in eukaryotes are also proteolytic substrates and their degradation is regulated in a similar way to what we report here for the *E. coli* proteins. The yeast NEF2, consisting of Rad4 and Rad23 proteins, binds preferentially to UV-damaged DNA. The Rad4 protein is degraded by the 26S proteasome in damaged yeast cells, and Rad23 is critical for protection of Rad4 against degradation (Lommel *et al.*, 2002; Ortolan *et al.*, 2004; Gillette *et al.*, 2006). The human XPC protein, which is a component of the XPC-hHR23 protein complex (a human homolog of budding yeast Rad4-Rad23), is also degraded upon UV-irradiation (Wang *et al.*, 2007) and interestingly, XPC is stabilized by its association with a second repair protein, HR23 (Ng *et al.*, 2003; Okuda *et al.*, 2004). Furthermore, the rate of XPC protein synthesis is also induced following UV-irradiation. Thus, an interestingly common theme emerges: in *E. coli*, yeast and mammals, the “distortion recognition factors” involved in the critical early recognition step of repair (UvrA in *E. coli*, Rad4 in yeast, and XPC in mammals) are subjected to degradation and stabilized by interacting partner proteins (UvrB, Rad23 and HR23, respectively).

The fate of other DNA damage repair proteins following DNA insults

The cells likely need to actively rid themselves of UvrA as the DNA damage is resolved because the UvrABC proteins can also incise the undamaged DNA and can be a source of spontaneous mutations (Caron and Grossman, 1988; Branum *et al.*, 2001; Hasegawa *et al.*, 2008). It is also metabolically expensive to keep proteins at high concentrations when the cells do not need them. However, it has been thus far not possible to test the hypothesis that failure to degrade UvrA is mutagenic directly, as *clpX* mutants affect the stability of numerous SOS-regulated proteins, including the components of the "mutagenic" lesion bypass polymerase (PolV) (Frank *et al.*, 1996; Gonzalez *et al.*, 2000; Neher *et al.*, 2003b), and we have not succeeded in identifying the degradation signals on UvrA, and therefore cannot yet construct an "undegradable allele".

Is UvrA degradation likely to be sufficient to avoid the attack of undamaged DNA? What happens with the UvrA interacting proteins or other DNA repair proteins after the damage has been repaired? Studies done by Lin *et al.*, 1997 show that in *E. coli* UvrB protein levels increase following UV exposure and decrease during recovery. This result suggests that proteolysis may also regulate the UvrB levels. UvrC, Mfd and RecN were found to be tmRNA substrates in *Caulobacter crescentus*, and thus likely to exist in a form that is rapidly degraded at least under some conditions as the tmRNA-encoded peptide tag contains recognition sites for several intracellular proteases (Keiler *et al.*, 1996; Gottesman *et al.*, 1998; Herman *et al.*, 1998; Hong *et al.*, 2007). RecN, required for double strand breaks repair, is a ClpXP substrate and the degradation of cytoplasmic RecN aggregates after release from DNA damage is important for cell viability (Nagashima *et al.*, 2006; Neher *et al.*, 2006). ClpXP protease is also required for radioresistance in *Deinococcus radiodurans* and controls chromosome segregation and cell division in cells recovering from γ-irradiation (Servant *et al.*, 2007). Thus, it is likely that we have a very incomplete picture of the extent to which proteolysis, and other protein quality control pathways play a role in the complex dynamics of the DNA damage response.

EXPERIMENTAL PROCEDURES

Bacterial strains and growth conditions

Strain MC4100 or MC4100 derivatives were grown at 37°C in Luria-Bertani or M9 minimal medium supplemented with 0.4% glucose as a carbon source. Growth was monitored by measuring the optical density at 600 nm (OD_{600}). For plasmid-carrying strains and for selecting transductants, various antibiotics were added to the growth medium as recommended (Miller, 1972).

Construction of *uvrA, uvrB and mfd* deletion mutants

The MC4100 *uvrA*, *uvrB* and *mfd* mutants were constructed by one-step inactivation using the λ Red system (Datsenko and Wanner, 2000). The chromosomal *uvrA*, *uvrB* or *mfd* gene was deleted and replaced with *cat* cassette generated by PCR using pKD3 DNA as a template. The primers employed contained homology extensions to the noncoding regions located upstream and downstream of the respective genes and were as follows:

5'-gctggtgcaactctgaaaggaaaaggccgctcagaaagcgtgtaggctggagctgcttc-3';

5'-catgccaccgggcaaaaaagcgtttaatccgggaaaggtgacatatgaatatcctccttagt-3' (*uvrA* mutant), 5'-gtatcagaaatattatggtgatgaactgtttttttatccgtgtaggctggagctgcttc-3';

5'-gctgttttccgtttgtcatcagtcttcttcgctatcctgcatatgaatatcctccttagt-3' (*uvrB* mutant), and 5'-gtaaatgttgcagatgggggcgcagaaacgccccgatttacgtgtaggctggagctgcttc-3';

5'-ccatatgttgaggcatatcctaacgagaatctgacaaccgtcatatgaatatcctccttagt-3' (*mfd* mutant).

The correct replacement of the open reading frames by the *cat* gene was confirmed by PCR as described (Datsenko and Wanner, 2000).

Generation of *uvrC^{D399A} allele*

The *uvrC^{D399A}* mutation was constructed using recombineering (Thomason *et al.*, 2007). A PCR fragment containing D399A replacement was generated by site-directed mutagenesis using a four-primer two-step PCR procedure (Germer *et al.*, 2001). As 'internal' primers

5'-gctgat**ag**caaagcactccatc-3' and

5'-gatggagtgctttg**ct**atcagc-3'

were used to create a double point mutation in the *uvrC* coding region (the altered nucleotides are bold) and the 'external' primers were

5'-caatggtttccagggaactggtatttttgaccttcgcccgtttttttac-3' (UvrC-H1 homology sequence) and

5'-caggcggtgcgacgcgtcaccgaaaaacaattcgtttccaatac-3' (UvrC-H2 homology sequence).

DY441 chromosomal DNA and the primers

5'- caatggtttccagggaactggtatttttgaccttcgcccgtttttttactgtgacggaagatcacttcg-3' (UvrC-H1-*cat*) and

5'-caggcggtgcgacgcgtcaccgaaaaacaattcgtttccaatacatcaaagggaaaactgtccatat-3' (UvrC-H2-*sacB*)

were used to generate the H1-*cat-sacB*-H2 PCR fragment. This PCR fragment was electroporated into MC4100 cells carrying the temperature sensitive pSIM6 (Amp^R) with the λ *red* genes, selecting for Cm resistance (Cm^R) colonies and testing for sensitivity to sucrose. A confirmed Cm^R/sucrose-sensitive candidate (containing the *cat-sacB* in the *uvrC* coding region in the chromosome) was used for electroporation of the *uvrC^{D399A}* PCR fragment, selecting for sucrose-resistance colonies and then testing for Cm^S. In these colonies the *cat-sacB* cassette was replaced with *uvrC^{D399A}*. Plasmid curing was performed as described (Datta *et al.*, 2006). The D399A replacement was confirmed by colony PCR followed by DNA sequencing.

Expression and purification of untagged UvrA protein

The *uvrA* coding region was amplified from chromosomal DNA by PCR using the primers

5'- gtttaatccgggaaaggcatatggataagatcgaag-3' (NdeI) and

5'- cagaaaggatccttaacgattacagcatcggcttaagg-3' (BamHI).

The NdeI/BamHI-cut PCR fragment was cloned into digested pET11a (Novagen), resulting in pMP47. pMP47 was transformed into the bacterial strain BL21(DE3) carrying the pLysS plasmid (Novagen). Cells were grown in LB with ampicillin (100 μg ml^{-1}) and chloramphenicol (30 μg ml^{-1}) at 30°C to an OD_{600} of 0.6 before IPTG was added. After a 4 h induction, the cells from a 3-liter culture were harvested and UvrA was purified as described (Thomas *et al.*, 1985) with a few modifications. The pellet was resuspended in buffer A (50 mM Tris pH 8, 100 mM NaCl, 1 mM EDTA, 10 mM β-mercaptoethanol), and the cells were disrupted by French press. The whole cell extract was centrifuged for 30 min at 19000 rpm (Sorvall SS-34 rotor) and Polymin P (10%, pH 8) was added to the supernantant as described, followed by precipitation with 35% and 65% ammonium sulfate. After dissolving the precipitate in 10 ml buffer B (50 mM Tris pH 7.5, 100 mM NaCl, 10 mM β-mercaptoethanol, 1 mM EDTA, 20% glycerol), the sample was desalted (PD10 column) and loaded onto a Source Q column. The column was developed with a 102 ml

gradient of 100-400 mM KCl. The fractions containing the UvrA protein were pooled and desalted onto PD-10 columns. The desalted sample was loaded onto a Hi-Trap Heparin column (1 ml) equilibrated in buffer B and developed with a 20 ml gradient 0.1-2 M KCl. The UvrA containing fractions were pooled, desalted/exchanged (PD-10 column) into buffer B and concentrated to 10 μM with an Amicon Ultra-4 (30 KDa MWCO) concentrator.

Purification of His_6-tagged UvrA, UvrB and production of polyclonal antibodies against UvrA

pET23b (Novagen, CmR) carrying a T7 IPTG-inducible promoter was used for cloning the C-terminally polyhistidine (6xHis)-tagged variant of UvrA. The *uvrA* coding region was amplified from chromosomal DNA by PCR using the primers:

5'- gtttaatccgggaaaggcatatggataagatcgaag-3' (NdeI) and

5'- gaaagcggccttaacgactcgagcatcggcttaagg -3' (XhoI).

This PCR fragment was NdeI/XhoI cleaved and ligated into digested pET23b (resulting in pMP46). For the N-terminally (6xHis)-tagged variant of UvrB a *uvrB*-coding PCR fragment was digested with NdeI and XhoI restriction enzymes and cloned into digested pET28b (Novagen, Kan^R), resulting in pMP50. The primers used were

5'- ggtagcgacatatgagtaaaccgttcaaactg -3' (NdeI) and

5'- cttcgctctcgagttacgatgccgcgataaacagc -3' (XhoI).

BL21(DE3) carrying the pLysS (Novagen) and pMP46 or pMP50 plasmids was used for expression of UvrA or UvrB. Cells were grown in LB with ampicillin (100 μg ml^{-1}) or kanamycin (50 μg ml^{-1}), and chloramphenicol (30 μg ml^{-1}) at 30°C to an OD_{600} of 0.6 before IPTG was added. After a 3-h induction, the cells from a 2-liter culture were harvested and disrupted by French press. The eluted proteins from the nickel-NTA columns were loaded onto a Sephacryl S-100 High Resolution gel filtration column equilibrated in UvrA storage buffer (50 mM Tris pH 7.5, 300 mM NaCl, 1 mM EDTA, 1 mM DTT, 10% glycerol) or UvrB storage buffer (50 mM Tris pH 7.5, 100 mM NaCl, 10 mM β-mercaptoethanol, 1 mM EDTA, 20% glycerol). Samples with a protein concentration of 10 μM 6xHis-tagged UvrA were used for rabbit polyclonal antibody production (Covance Research Products).

Pulse-chase labeling and immunoprecipitation

Pulse-labeling of cells with L-[^{35}S]-methionine and immunoprecipitation was performed as described previously (Lange and Hengge-Aronis, 1994). For the determination of the UvrA rate of synthesis 1-ml samples were taken before and after DNA damage, and the optical density was adjusted to OD_{600} of 0.3 with supernatant from their own culture obtained by filter sterilization immediately before taking the samples. The cultures were grown in M9 minimal medium containing 0.4% glucose and exponentially growing cells were harvested and pulse-labeled for 2 min, followed by chase times between 30 seconds and 150 min. Polyclonal sera against UvrA were used for immunoprecipitation. Immunoprecipitated proteins were quantified directly from the dried gels using a Typhoon scanner and ImageQuant software (Amersham Biosciences).

Gel electrophoresis and Western blotting

Sample for SDS-polyacrylamide gel electrophoresis and immunoblot analysis were taken before and after DNA damage (during post-UV recovery). Following the addition of ice cold trichloroacetic acid to 10%, the samples were harvested by centrifugation, washed with 100% acetone, and resuspended in SDS loading buffer to an OD_{600} of 10. The protein levels were detected by western blot using polyclonal antibodies against UvrA and ECF detection

(Amersham). Band intensity was imaged and quantified using a Typhoon scanner and ImageQuant software (Amersham Biosciences).

UV-irradiation

Strain MC4100 or MC4100 derivatives were grown at 37°C in M9 minimal medium supplemented with 0.4% glucose. At an OD_{600} of 0.3, 15 ml cultures were UV-irradiated (UV dose 10J/m^2) in Petri plates, using a 15W G15T8 germicidal lamp (GE), and then return to flasks for further growth. The UV intensity was measured using a UVX radiometer (UVP).

Enzyme-linked immunosorbent assay (ELISA) for cyclobutane pyrimidine dimers (CPDs)

The content of CPDs was determined using chromosomal DNA and TDM-2 anti-CPDs antibodies according to the manufacturer's protocol (MBL International Corporation). Chromosomal DNA was prepared (using Qiagen DNeasy Blood & Tissue Kit) from 1 ml samples removed immediately after UV exposure or at specific times during post-UV recovery. 10 ng DNA was coated to the microtiter plates precoated with protamine sulfate and after adding TDM-2 antibodies, biotinylated F $(ab')_2$ anti-mouse IgG fragments and streptavidin-peroxidase, the absorbance of colored products from hydrogen peroxide-oxidation of o-Phenylene diamine was measured at 492 nm.

Supplementary Material

Refer to Web version on PubMed Central for supplementary material.

Acknowledgments

We thank members of the Baker and Sauer laboratories for helpful discussions, Walker lab for use of equipment, and in particular Susan Cohen for many discussions and advice. We are grateful to Donald L. Court for providing the plasmid pSIM6 and the DY441 bacterial strain, and to Susan Cohen and Kevin Wang for critical reading of the manuscript. This work was supported by NIH grant GM49224. T.A.B. and M.P. are employees of the Howard Hughes Medical Institute.

References

Assenmacher N, Wenig K, Lammens A, Hopfner KP. Structural basis for transcription-coupled repair: the N terminus of Mfd resembles UvrB with degenerate ATPase motifs. J Mol Biol. 2006; 355:675–683. [PubMed: 16309703]

Branum ME, Reardon JT, Sancar A. DNA repair excision nuclease attacks undamaged DNA. A potential source of spontaneous mutations. J Biol Chem. 2001; 276:25421–25426. [PubMed: 11353769]

Cadet J, Anselmino C, Douki T, Voituriez L. Photochemistry of nucleic acids in cells. J Photochem Photobiol B. 1992; 15:277–298. [PubMed: 1432396]

Caron PR, Grossman L. Incision of damaged versus nondamaged DNA by the *Escherichia coli* UvrABC proteins. Nucleic Acids Res. 1988; 16:7855–7865. [PubMed: 2843804]

Chandrasekhar D, Van Houten B. In vivo formation and repair of cyclobutane pyrimidine dimers and 6-4 photoproducts measured at the gene and nucleotide level in *Escherichia coli*. Mutat Res. 2000; 450:19–40. [PubMed: 10838132]

Cleaver JE. Photoreactivation. DNA Repair (Amst). 2003; 2:629, 637–628. [PubMed: 12713819]

Courcelle J, Khodursky A, Peter B, Brown PO, Hanawalt PC. Comparative gene expression profiles following UV exposure in wild-type and SOS-deficient *Escherichia coli*. Genetics. 2001; 158:41–64. [PubMed: 11333217]

Datsenko KA, Wanner BL. One-step inactivation of chromosomal genes in *Escherichia coli* K-12 using PCR products. Proc Natl Acad Sci U S A. 2000; 97:6640–6645. [PubMed: 10829079]

Datta S, Costantino N, Court DL. A set of recombineering plasmids for gram-negative bacteria. Gene. 2006; 379:109–115. [PubMed: 16750601]

Deaconescu AM, Chambers AL, Smith AJ, Nickels BE, Hochschild A, Savery NJ, Darst SA. Structural basis for bacterial transcription-coupled DNA repair. Cell. 2006; 124:507–520. [PubMed: 16469698]

Fernandez De Henestrosa AR, Ogi T, Aoyagi S, Chafin D, Hayes JJ, Ohmori H, Woodgate R. Identification of additional genes belonging to the LexA regulon in *Escherichia coli*. Mol Microbiol. 2000; 35:1560–1572. [PubMed: 10760155]

Frank EG, Ennis DG, Gonzalez M, Levine AS, Woodgate R. Regulation of SOS mutagenesis by proteolysis. Proc Natl Acad Sci U S A. 1996; 93:10291–10296. [PubMed: 8816793]

Friedberg, EC.; Walker, GC.; Siede, W.; Wood, RD.; Schultz, RA.; Ellenberger, T. DNA repair and mutagenesis. Second Edition. American Society for Microbiology; Washington, D.C: 2005.

Germer J, Becker G, Metzner M, Hengge-Aronis R. Role of activator site position and a distal UP-element half-site for sigma factor selectivity at a CRP/H-NS-activated sigma(s)-dependent promoter in *Escherichia coli*. Mol Microbiol. 2001; 41:705–16. [PubMed: 11532138]

Gillette TG, Yu S, Zhou Z, Waters R, Johnston SA, Reed SH. Distinct functions of the ubiquitin-proteasome pathway influence nucleotide excision repair. EMBO J. 2006; 25:2529–2538. [PubMed: 16675952]

Gonzalez M, Rasulova F, Maurizi MR, Woodgate R. Subunit-specific degradation of the UmuD/D' heterodimer by the ClpXP protease: the role of trans recognition in UmuD' stability. EMBO J. 2000; 19:5251–5258. [PubMed: 11013227]

Gottesman S, Roche E, Zhou Y, Sauer RT. The ClpXP and ClpAP proteases degrade proteins with carboxy-terminal peptide tails added by the SsrA-tagging system. Genes Dev. 1998; 12:1338–1347. [PubMed: 9573050]

Gottesman S. Proteolysis in bacterial regulatory circuits. Annu Rev Cell Dev Biol. 2003; 19:565–587. [PubMed: 14570582]

Hanson PI, Whiteheart SW. AAA+ proteins: have engine, will work. Nat Rev Mol Cell Biol. 2005; 6:519–529. [PubMed: 16072036]

Hasegawa K, Yoshiyama K, Maki K. Spontaneous mutagenesis associated with nucleotide excision repair in Escherichia coli. Genes to Cells. 2008; 13:459–469. [PubMed: 18429818]

Herman C, Thevenet D, Bouloc P, Walker GC, D'Ari R. Degradation of carboxy-terminal-tagged cytoplasmic proteins by the *Escherichia coli* protease HflB (FtsH). Genes Dev. 1998; 12:1348–1355. [PubMed: 9573051]

Hong SJ, Lessner FH, Mahen EM, Keiler KC. Proteomic identification of tmRNA substrates. Proc Natl Acad Sci U S A. 2007; 104:17128–17133. [PubMed: 17940001]

Hoskins JR, Wickner S. Two peptide sequences can function cooperatively to facilitate binding and unfolding by ClpA and degradation by ClpAP. Proc Natl Acad Sci U S A. 2006; 103:909–914. [PubMed: 16410355]

Jenal U, Hengge-Aronis R. Regulation by proteolysis in bacterial cells. Curr Opin Microbiol. 2003; 6:163–172. [PubMed: 12732307]

Keiler KC, Waller PR, Sauer RT. Role of a peptide tagging system in degradation of proteins synthesized from damaged messenger RNA. Science. 1996; 271:990–993. [PubMed: 8584937]

Kelner A. Action spectra for photoreactivation of ultraviolet-irradiated Escherichia coli and Streptomyces griseus. J Gen Physiol. 1951; 34:835–852. [PubMed: 14850704]

Kenyon CJ, Walker GC. Expression of the *E. coli* uvrA gene is inducible. Nature. 1981; 289:808–810. [PubMed: 6780917]

Lange R, Hengge-Aronis R. The cellular concentration of the sigma S subunit of RNA polymerase in *Escherichia coli* is controlled at the levels of transcription, translation, and protein stability. Genes Dev. 1994; 8:1600–1612. [PubMed: 7525405]

Lin CG, Kovalsky O, Grossman L. DNA damage-dependent recruitment of nucleotide excision repair and transcription proteins to *Escherichia coli* inner membranes. Nucleic Acids Res. 1997; 25:3151–3158. [PubMed: 9304113]

Lin JJ, Sancar A. Active site of (A)BC excinuclease. I. Evidence for 5' incision by UvrC through a catalytic site involving Asp399, Asp438, Asp466, and His538 residues. J Biol Chem. 1992; 267:17688–17692. [PubMed: 1387639]

Little, JW. Variations in the in vivo stability of LexA repressor during the SOS regulatory cycle. In: Friedberg, EC.; Bridges, BA., editors. Cellular Responses to DNA Damage. New York: Alan Liss; 1983. p. 269-378.

Lommel L, Ortolan T, Chen L, Madura K, Sweder KS. Proteolysis of a nucleotide excision repair protein by the 26 S proteasome. Curr Genet. 2002; 42:9–20. [PubMed: 12420141]

Malta E, Moolenaar GF, Goosen N. Dynamics of the UvrABC nucleotide excision repair proteins analyzed by fluorescence resonance energy transfer. Biochemistry. 2007; 46:9080–9088. [PubMed: 17630776]

Mellon I, Hanawalt PC. Induction of the *Escherichia coli* lactose operon selectively increases repair of its transcribed DNA strand. Nature. 1989; 342:95–98. [PubMed: 2554145]

Mellon I. Transcription-coupled repair: a complex affair. Mutat Res. 2005; 577:155–161. [PubMed: 15913669]

Miller, JH. Experiments in molecular genetics. Cold Spring harbor N.Y.: Cold Spring Harbor Laboratory; 1972.

Mizusawa S, Gottesman S. Protein degradation in *Escherichia coli*: the *lon* gene controls the stability of sulA protein. Proc Natl Acad Sci U S A. 1983; 80:358–362. [PubMed: 6300834]

Moolenaar GF, van Rossum-Fikkert S, van Kesteren M, Goosen N. Cho, a second endonuclease involved in *Escherichia coli* nucleotide excision repair. Proc Natl Acad Sci U S A. 2002; 99:1467–1472. [PubMed: 11818552]

Nagashima K, Kubota Y, Shibata T, Sakaguchi C, Shinagawa H, Hishida T. Degradation of *Escherichia coli* RecN aggregates by ClpXP protease and its implications for DNA damage tolerance. J Biol Chem. 2006; 281:30941–30946. [PubMed: 16914543]

Neher SB, Flynn JM, Sauer RT, Baker TA. Latent ClpX-recognition signals ensure LexA destruction after DNA damage. Genes Dev. 2003a; 17:1084–1089. [PubMed: 12730132]

Neher SB, Sauer RT, Baker TA. Distinct peptide signals in the UmuD and UmuD' subunits of UmuD/D' mediate tethering and substrate processing by the ClpXP protease. Proc Natl Acad Sci U S A. 2003b; 100:13219–13224. [PubMed: 14595014]

Neher SB, Villen J, Oakes EC, Bakalarski CE, Sauer RT, Gygi SP, Baker TA. Proteomic profiling of ClpXP substrates after DNA damage reveals extensive instability within SOS regulon. Mol Cell. 2006; 22:193–204. [PubMed: 16630889]

Ng JM, Vermeulen W, van der Horst GT, Bergink S, Sugasawa K, Vrieling H, Hoeijmakers JH. A novel regulation mechanism of DNA repair by damage-induced and RAD23-dependent stabilization of xeroderma pigmentosum group C protein. Genes Dev. 2003; 17:1630–1645. [PubMed: 12815074]

Okuda Y, Nishi R, Ng JM, Vermeulen W, van der Horst GT, Mori T, et al. Relative levels of the two mammalian Rad23 homologs determine composition and stability of the xeroderma pigmentosum group C protein complex. DNA Repair (Amst). 2004; 3:1285–1295. [PubMed: 15336624]

Orren DK, Sancar A. The (A)BC excinuclease of *Escherichia coli* has only the UvrB and UvrC subunits in the incision complex. Proc Natl Acad Sci U S A. 1989; 86:5237–5241. [PubMed: 2546148]

Ortolan TG, Chen L, Tongaonkar P, Madura K. Rad23 stabilizes Rad4 from degradation by the Ub/proteasome pathway. Nucleic Acids Res. 2004; 32:6490–6500. [PubMed: 15601997]

Pakotiprapha D, Inuzuka Y, Bowman BR, Moolenaar GF, Goosen N, Jeruzalmi D, Verdine GL. Crystal structure of *Bacillus stearothermophilus* UvrA provides insight into ATP-modulated dimerization, UvrB interaction, and DNA binding. Mol Cell. 2008; 29:122–133. [PubMed: 18158267]

Prakash S, Tian L, Ratliff KS, Lehotzky RE, Matouschek A. An unstructured initiation site is required for efficient proteasome-mediated degradation. Nat Struct Mol Biol. 2004; 11:830–837. [PubMed: 15311270]

Roberts J, Park JS. Mfd, the bacterial transcription repair coupling factor: translocation, repair and termination. Curr Opin Microbiol. 2004; 7:120–125. [PubMed: 15063847]

Sancar A, Rupp WD. A novel repair enzyme: UVRABC excision nuclease of *Escherichia coli* cuts a DNA strand on both sides of the damaged region. Cell. 1983; 33:249–260. [PubMed: 6380755]

Sancar A. DNA excision repair. Annu Rev Biochem. 1996; 65:43–81. [PubMed: 8811174]

Sauer RT, Bolon DN, Burton BM, Burton RE, Flynn JM, Grant RA, et al. Sculpting the proteome with AAA(+) proteases and disassembly machines. Cell. 2004; 119:9–18. [PubMed: 15454077]

Savery NJ. The molecular mechanism of transcription-coupled DNA repair. Trends Microbiol. 2007; 15:326–333. [PubMed: 17572090]

Selby CP, Sancar A. Gene- and strand-specific repair in vitro: partial purification of a transcription-repair coupling factor. Proc Natl Acad Sci U S A. 1991; 88:8232–8236. [PubMed: 1896474]

Selby CP, Witkin EM, Sancar A. *Escherichia coli* mfd mutant deficient in “mutation frequency decline” lacks strand-specific repair: in vitro complementation with purified coupling factor. Proc Natl Acad Sci U S A. 1991; 88:11574–11578. [PubMed: 1763073]

Selby CP, Sancar A. Structure and function of transcription-repair coupling factor. I. Structural domains and binding properties. J Biol Chem. 1995; 270:4882–4889. [PubMed: 7876261]

Servant P, Jolivet E, Bentchikou E, Mennecier S, Bailone A, Sommer S. The ClpPX protease is required for radioresistance and regulates cell division after gamma-irradiation in *Deinococcus radiodurans*. Mol Microbiol. 2007; 66:1231–1239. [PubMed: 17986186]

Theis K, Skorvaga M, Machius M, Nakagawa N, Van Houten B, Kisker C. The nucleotide excision repair protein UvrB, a helicase-like enzyme with a catch. Mutat Res. 2000; 460:277–300. [PubMed: 10946234]

Thomas DC, Levy M, Sancar A. Amplification and purification of UvrA, UvrB, and UvrC proteins of *Escherichia coli*. J Biol Chem. 1985; 260:9875–9883. [PubMed: 2991268]

Thomason L, Court DL, Bubunenko M, Costantino N, Wilson H, Datta S, Oppenheim A. Recombineering: genetic engineering in bacteria using homologous recombination. Curr Protoc Mol Biol. 2007; Chapter 1:Unit 1–16.

Thompson CL, Sancar A. Photolyase/cryptochrome blue-light photoreceptors use photon energy to repair DNA and reset the circadian clock. Oncogene. 2002; 21:9043–9056. [PubMed: 12483519]

Truglio JJ, Croteau DL, Skorvaga M, DellaVecchia MJ, Theis K, Mandavilli BS, et al. Interactions between UvrA and UvrB: the role of UvrB’s domain 2 in nucleotide excision repair. EMBO J. 2004; 23:2498–2509. [PubMed: 15192705]

Truglio JJ, Croteau DL, Van Houten B, Kisker C. Prokaryotic nucleotide excision repair: the UvrABC system. Chem Rev. 2006; 106:233–252. [PubMed: 16464004]

Van Houten B, Croteau DL, DellaVecchia MJ, Wang H, Kisker C. ‘Close-fitting sleeves’: DNA damage recognition by the UvrABC nuclease system. Mutat Res. 2005; 577:92–117. [PubMed: 15927210]

Verhoeven EE, van Kesteren M, Moolenaar GF, Visse R, Goosen N. Catalytic sites for 3’ and 5’ incision of *Escherichia coli* nucleotide excision repair are both located in UvrC. J Biol Chem. 2000; 275:5120–5123. [PubMed: 10671556]

Verhoeven EE, Wyman C, Moolenaar GF, Goosen N. The presence of two UvrB subunits in the UvrAB complex ensures damage detection in both DNA strands. EMBO J. 2002; 21:4196–4205. [PubMed: 12145219]

Walker, GC.; Smith, BT.; Sutton, MD. The SOS response to DNA damage. In: Storz, G.; Hengge-Aronis, R., editors. Bacterial Stress Responses. Washington, DC: American Society for Microbiology Press; 2000. p. 131-144.

Wang QE, Praetorius-Ibba M, Zhu Q, El-Mahdy MA, Wani G, Zhao Q, et al. Ubiquitylation-independent degradation of Xeroderma pigmentosum group C protein is required for efficient nucleotide excision repair. Nucleic Acids Res. 2007; 35:5338–5350. [PubMed: 17693435]

Wu WF, Zhou Y, Gottesman S. Redundant in vivo proteolytic activities of *Escherichia coli* Lon and the ClpYQ (HslUV) protease. J Bacteriol. 1999; 181:3681–3687. [PubMed: 10368141]

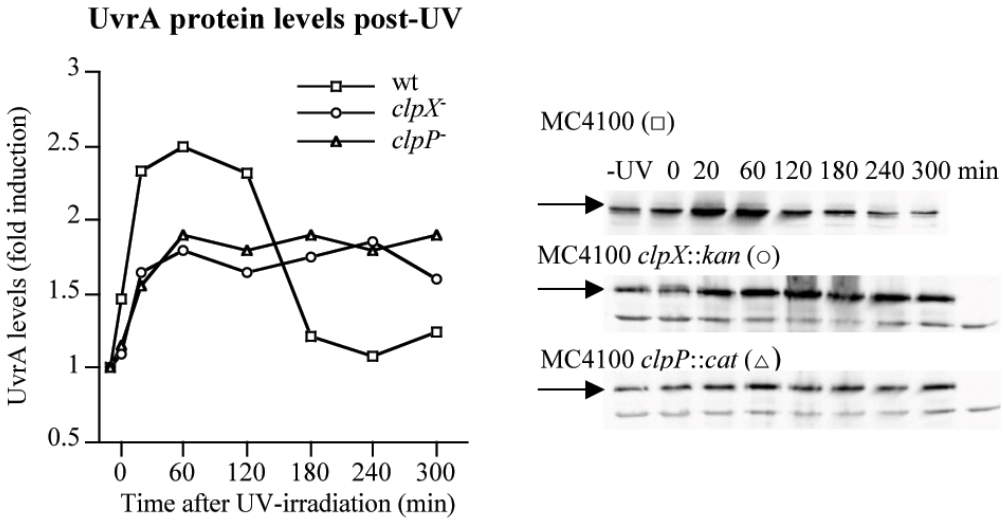

FIGURE 1. UvrA protein levels before and after UV-irradiation in wild-type, *clpX* and *clpP* mutant cells

Samples for western blots were removed at specific time points during recovery growth of MC4100 (squares) and its *clpX*::*kan* (circles) or *clpP*::*cat* (triangles) derivatives. In the last lanes samples from an MC4100 *uvrA*::*cat* derivative were loaded as a control. UvrA protein levels (marked with arrows) were quantified, normalized against the levels before UV-irradiation in each strain, and represented as fold induction. The data points are the average of three independent experiments. The protein band below UvrA was used as an internal control. Experiments with *uvrA*$^{-}$ cells reveal that this protein is unrelated to UvrA, and quantification of this band reveals no evidence that this protein is itself unstable.

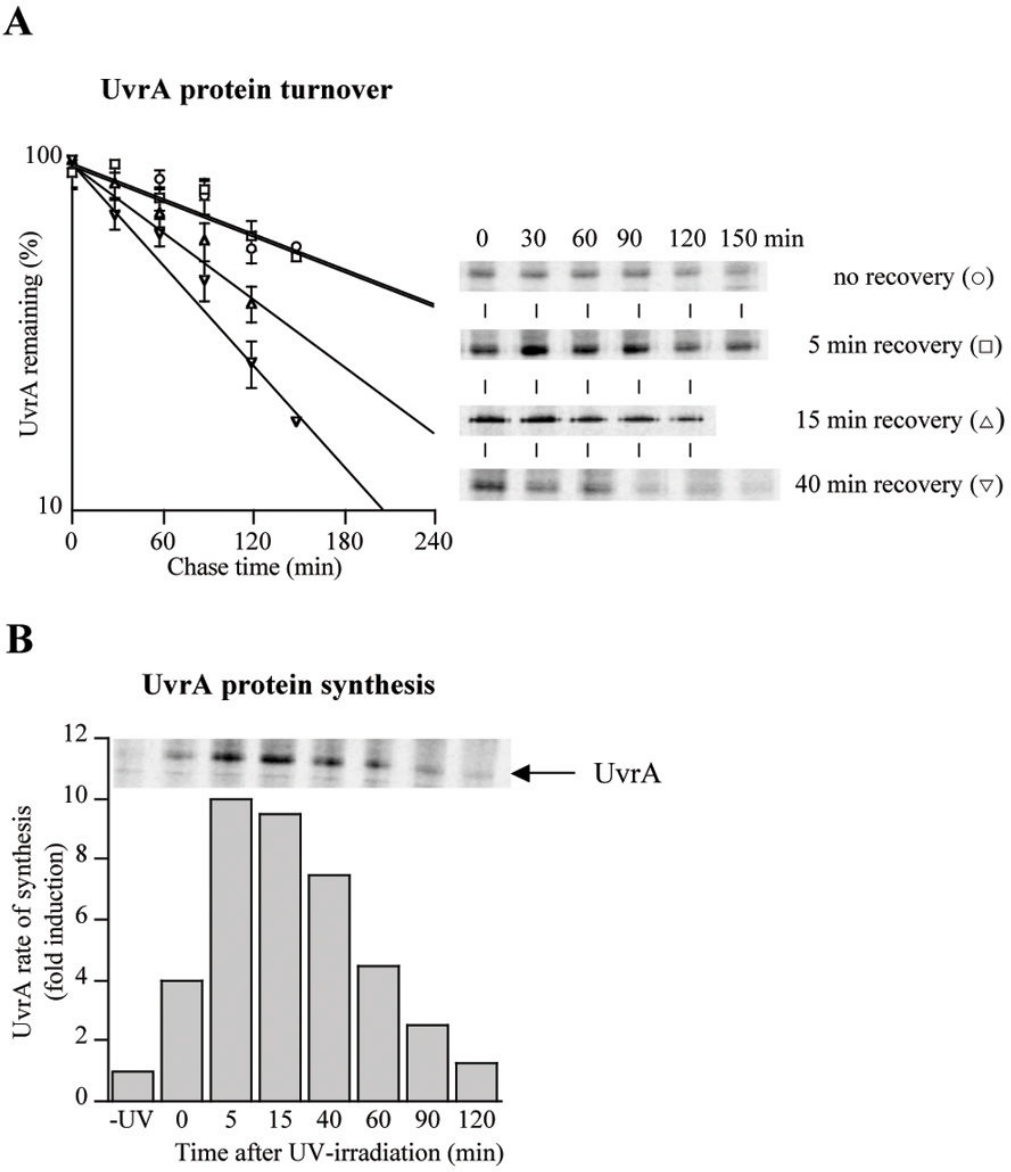

FIGURE 2. UvrA degradation and synthesis during post-UV recovery

A. Wild-type cells were treated with UV and either immediately labeled (circles in A) or at the following time points during recovery: 5 min (squares in A), 15 min (triangles in A) and 40 min recovery (inverted triangles in A). UvrA proteolysis was measured by pulse-chase labeling and UvrA immunoprecipitation, and the original phosphoimager data are shown in A. Final data obtained from quantitative phosphoimager analysis represent the average of four independent experiments with the error bars indicating the standard deviation. ***B.*** UvrA rate of synthesis was measured before and after UV-irradiation.

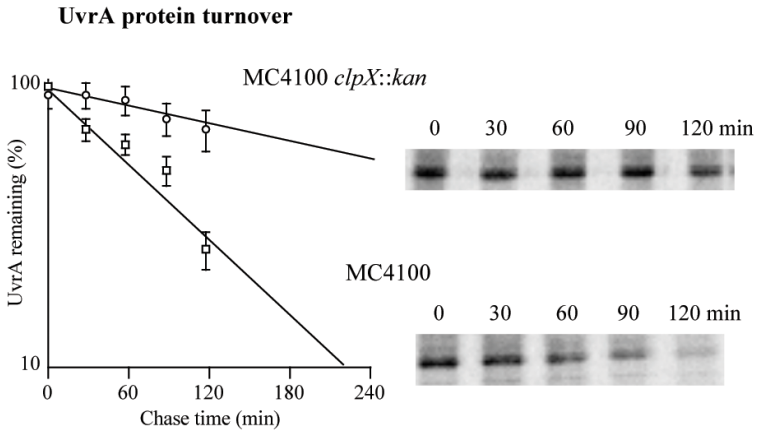

FIGURE 3. UvrA stability in *clpX* mutant cells

MC4100 (squares) and its *clpX::kan* (circles) derivative were allowed to recover for 40 min after UV-irradiation, and then were pulse-chase labeled to measure UvrA proteolysis. Original phosphoimager data and the data from quantitative phosphoimager analysis are shown. The data points represent the average of four independent experiments with the error bars indicating the standard deviation.

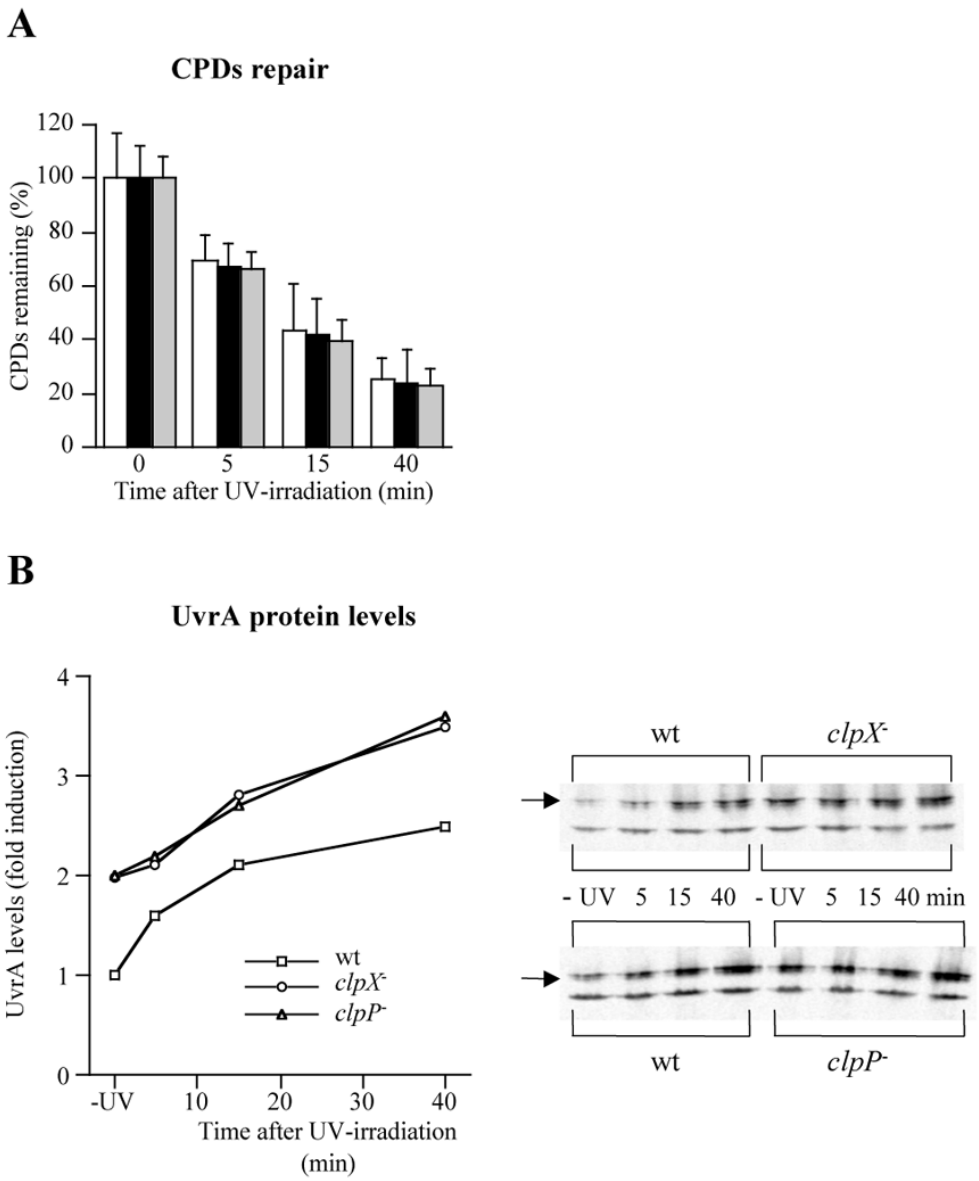

FIGURE 4. CPDs repair in wild-type, *clpX* and *clpP* mutant cells after UV treatment

Purified chromosomal DNA from wild-type cells (white bars in A) and their *clpX::kan* (black bars in A) or *clpP::cat* (grey bars in A) derivatives was used to determined the CPDs content by direct ELISA. The data points represent the average of four independent experiments with the error bars indicating the standard deviation (A). UvrA levels in MC4100 (squares in B) and its *clpX::kan* (circles in B) or *clpP::cat* (triangles in B) derivatives were determined by western blot analysis from the same cultures used for the measurement of CPDs levels. UvrA levels (marked with arrows in B) were quantified, normalized against the levels in undamaged wild-type cells, and represented as fold induction. Each data point is the average of four independent experiments.

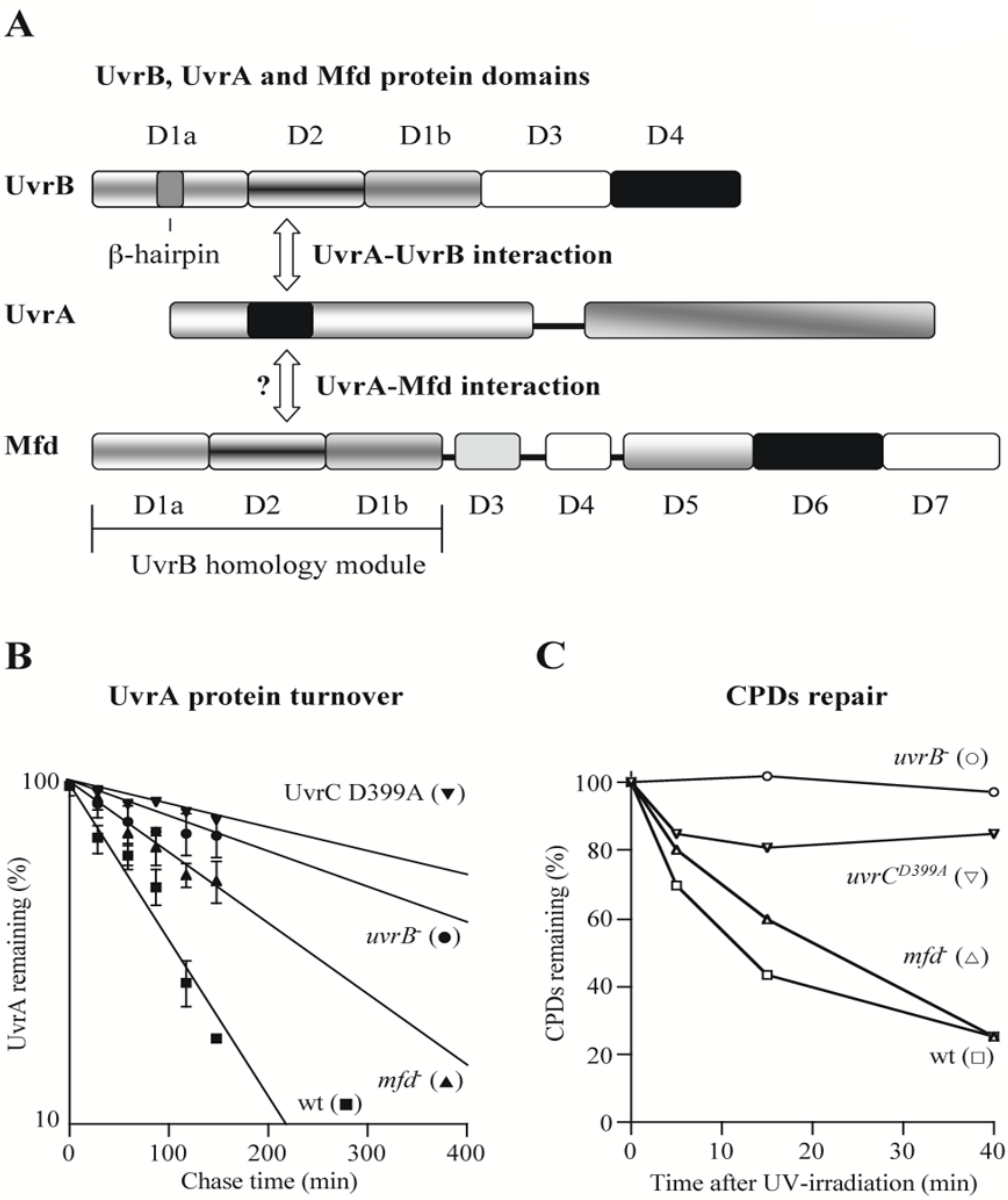

FIGURE 5. The effect of other NER components on UvrA proteolysis

A. Schematic representation of UvrB, UvrA and Mfd protein domains. The inserted segment (residues 118–257) in the nucleotide binding domain I of UvrA (shown in black) interacts with D2 of UvrB and the putative UvrA binding surface of Mfd is buried in the D2/D7 interface (Deaconescu *et al.*, 2006; Pakotiprapha *et al.*, 2008). There are no published data about the region in UvrA that interacts with Mfd. ***B.*** UvrA stability in *uvrB*, *mfd* and *uvrC*^{D399A} mutant cells. UvrA rate of degradation was determined in MC4100 (closed squares in B) and its *uvrB*::*cat* (closed circles in A), *mfd*::*cat* (closed triangles in B) and *uvrC*^{D399A} (closed inverted triangles in B) derivatives as described in the legend to Fig. 3. The data points represent the average of four independent experiments and the error bars indicate the standard deviations. ***C***. CPDs repair in MC4100, *uvrB*, *mfd* and *uvrC*^{D399A} mutant cells (open symbols).

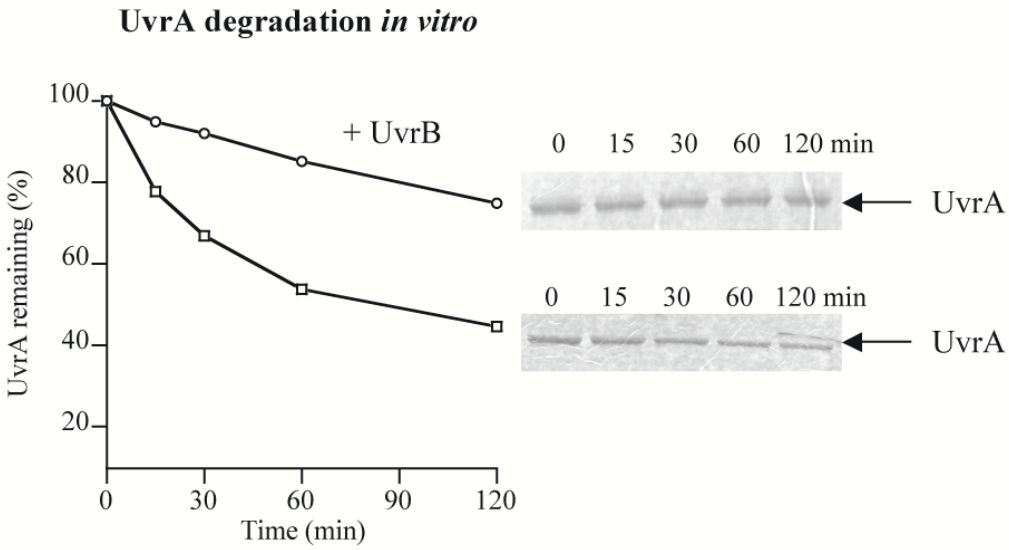

FIGURE 6. UvrB protects UvrA against degradation by ClpXP *in vitro*

UvrA degradation *in vitro* was performed at 30°C in PD buffer (25 mM Hepes-KOH pH 7.6, 5 mM KCl, 5 mM MgCl, 0.032% Nonidet P-40, 10% glycerol). The UvrA, UvrB, ClpX and ClpP were used at a final concentration of 1 μM in the presence of 10 nM undamaged DNA (pUC19) and an ATP regeneration system (16 mM creatine phosphate/0.32 mg/ml creatine kinase/5 mM ATP). Coomassie stained SDS-PAGE gels and final data from quantitative gel analysis are shown (squares-UvrA degradation in the absence of UvrB, circles-UvrA degradation in the presence of UvrB). Experiments were attempted using DNA that had been subjected to damaging UV-irradiation. This DNA did not stimulate ClpXP degradation of UvrA, however the results were not highly reproducible, and we suspect that the stabilizing affect of damaged DNA on UvrA involves a more complex set of components than is present in this *in vitro* reaction.

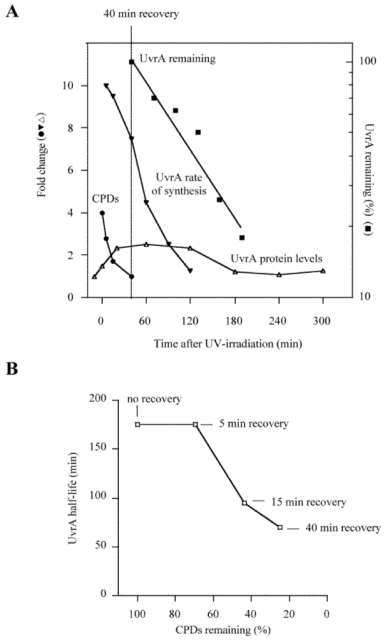

FIGURE 7. UvrA protein abundance is correlated with the persistence of CPDs in the cells

A. UvrA protein levels return to their basal level after the DNA damage has been repaired. UvrA levels (open triangles) increase approximately 2.5-fold following UV-irradiation. At the 40 min recovery time, when ~80% CPDs (closed circles) have been repaired, UvrA is degraded (closed squares) at the highest rate and the rate of UvrA synthesis (inverted triangles) declines significantly. ***B.*** The rate of UvrA degradation at distinct stages of recovery depends on the amount of unrepaired CPDs present in cells.